ISSN 1070-3284, Russian Journal of Coordination Chemistry, 2016, Vol. 42, No. 12, pp. 755–762. © Pleiades Publishing, Ltd., 2016.
Original Russian Text © D.A. Garnovskii, S.I. Levchenkov, G.G. Aleksandrov, N.I. Makarova, V.G. Vlasenko, Ya.V. Zubavichus, A.I. Uraev, A.A. Burlov, 2016, published in Koordinatsionnaya Khimiya, 2016, Vol. 42, No. 12, pp. 719–726.

Electrochemical and Chemical Syntheses, Structures, and Optical Properties of the Zinc and Cadmium Complexes in the N,N,O,S-Ligand Environment

D. A. Garnovskii[a, *], S. I. Levchenkov[a], G. G. Aleksandrov[b, †], N. I. Makarova[c], V. G. Vlasenko[d], Ya. V. Zubavichus[e], A. I. Uraev[c], and A. A. Burlov[c]

[a] *Southern Scientific Center, Russian Academy of Sciences, Rostov-on-Don, Russia*
[b] *Kurnakov Institute of General and Inorganic Chemistry, Russian Academy of Sciences, Moscow, 119991 Russia*
[c] *Research Institute of Physical and Organic Chemistry, Southern Federal University, Rostov-on-Don, Russia*
[d] *Research Institute of Physics, Southern Federal University, Rostov-on-Don, Russia*
[e] *Kurchatov Institute Russian Research Center, Moscow, 123182 Russia*
**e-mail: garn@ipoc.sfedu.ru*

Received April 1, 2016

Abstract—The chemical and electrochemical syntheses of the zinc (**I**) and cadmium (**II**) complexes are carried out on the basis of the tridentate Schiff base (H_2L), the condensation product of (2-tosylaminoaniline) *N*-(2-aminophenyl)-4-methylbenzenesulfunamide with 1-phenyl-3-methyl-4-formylpyrazole-5-thiol. The structures and compositions of the synthesized metallochelates are proved by the data of C, H, and N elemental analyses, IR spectroscopy, and ^{1}H NMR spectroscopy. X-ray absorption spectroscopy is used to determine the structure of the zinc complex. The binuclear structure of the cadmium complex is confirmed by the X-ray diffraction data (CIF file CCDC no. 1471159). The optical properties of H_2L and the zinc and cadmium complexes in dimethyl sulfoxide (DMSO) solutions are studied.

Keywords: electrosynthesis, N,N,S-tridentate Schiff base, metallochelates, binuclear complex, optical properties

DOI: 10.1134/S1070328416120010

INTRODUCTION

Many complexes with different structural, spectral, and magnetic properties were purposefully obtained depending on the denticity of potential azomethine ligand systems, condensation products of 1-phenyl-3-methyl-4-formylpyrazole-5-thiol and various aliphatic and aromatic amines, and on the nature of the complexing metal. The mononuclear chelates of zinc, cadmium, and nickel based on bidentate ligands with the tetrahedral configuration of the metal bonds undergo in solutions fast intramolecular stereoisomerization and intermolecular ligand exchange reactions [1, 2]. In addition, bidentate Schiff bases, 5-thiopyrazole aldehyde derivatives, are convenient objects for the directed synthesis of complexes with different *cis* or *trans* geometry of the MN_2S_2 chelate unit (M = Ni(II), Pd(II)) depending on the steric properties of the substituent at the N atom of the amine fragment of the ligand [3–9]. The mononuclear copper(II) complexes of bi- and tridentate thiopyrazole ligands with different N,S and N,S,O environments are very interesting, since they are convenient models for the interpretation of the structural, spectral, and electronic properties of the active centers of the "blue" copper proteins [10–14]. The low-spin iron thiolate complex based on the tridentate ligand, the condensation product of thiopyrazole aldehyde and 8-aminoquinoline with the $Fe(III)N_3S_3$ chelate mode, is a model of natural metalloenzyme nitrile hydratase [15]. The magnetic properties of the binuclear copper(II) complexes based on tri- and pentadentate azomethine ligands containing the thiopyrazole fragment were studied in several works [16–19].

This study is devoted to the synthesis of the zinc(II) and cadmium(II) chelates based on the N,N,S-sulfonamide pyrazole-containing tridentate Schiff bases, the study of their physicochemical properties and structures, and the comparison of the results of the electrochemical and chemical methods used for the synthesis of the metal complexes.

† Deceased.

EXPERIMENTAL

1-Phenyl-3-methyl-4-formylpyrazole-5-thiol and 2-tosylaminoaniline were synthesized using earlier described procedures [20, 21].

Synthesis of N-{2-[[3-methyl-1-phenyl-5-thioxopyrazol-4-idene]methyl]aminophenyl}-4-methylbenzenesulfonamide (H_2L). A solution of 2-tosylaminoaniline (1.05 g, 0.004 mol) in ethanol (10 mL) was added to a solution containing 1-phenyl-3-methyl-4-formylpyrazole-5-thiol (0.87 g, 0.004 mol) in ethanol (10 mL). The reaction mixture was refluxed for 2 h. A bright orange crystalline precipitate formed on cooling was filtered off, washed with hot isopropanol (10 mL), and dried in vacuo. The yield of the orange crystals of H_2L was 1.55 g (89%), mp = 171–172°C.

For $C_{24}H_{22}N_4O_2S_2$

anal. calcd., %:	C, 62.34;	H, 4.76;	N, 12.12.
Found, %:	C, 62.19;	H, 4.75;	N, 12.07.

IR (KBr), ν, cm^{-1}: 3183 w ν(N–H), 1638 s ν((C(=S)CH=CHN–), 1324 s $\nu_{as}(SO_2)$, 1154 s $\nu_s(SO_2)$. ^{1}H NMR (DMSO-d_6), δ, ppm: 2.40 (s, 3 H, CH_3), 2.43 (s, 3 H, CH_3), 6.68–8.04 (m, 13 H_{arom}), 8.67 (d, 1 H, C*H*–NH, ^3J = 12.4 Hz), 9.89 (s, 1 H, N–H), 14.49 (d, 1 H, CH–N*H*, ^3J = 12.4 Hz).

Chemical synthesis (CS) of the complexes. An equimolar amount of the corresponding zinc or cadmium acetate dihydrate dissolved in methanol (5 mL) was added to a boiling methanol–acetonitrile solution (15 mL) containing azomethine H_2L (0.00025 mol). After reflux for several hours, crystalline precipitates of the complexes formed on cooling were filtered off, washed with hot isopropanol, and dried in vacuo.

The yield of complex **I** in the form of bright yellow crystals was 0.168 g (64%), mp > 250°C.

For $C_{25}H_{24}N_4O_3S_2Zn$

anal. calcd., %:	C, 53.86;	H, 4.31;	N, 10.05.
Found, %:	C, 53.78;	H, 4.27;	N, 10.11.

IR (KBr), ν, cm^{-1}: 1618 s ν(C=N), 1254 s $\nu_{as}(SO_2)$, 1137 s $\nu_s(SO_2)$.

^{1}H NMR (DMSO-d_6), δ, ppm: 2.28 (s, 3 H, CH_3), 2.39 (s, 3 H, CH_3), 3.89 (q, 1 H, CH_3O*H*, ^3J = 14.7 Hz), 4.02 (d, 3 H, C*H*$_3$OH, ^3J = 14.7 Hz), 6.79–7.73 (m, 13 H_{arom}), 8.72 (s, 1 H, CH=N).

The yield of complex **II** in the form of yellow crystals was 0.196 g (65%), mp > 250°C.

For $C_{50}H_{48}N_8O_6S_4Cd_2$

anal. calcd., %:	C, 49.64;	H, 3.97;	N, 9.27.
Found, %:	C, 49.51;	H, 3.94;	N, 9.11.

IR (KBr), ν, cm^{-1}: 1612 s ν(C=N), 1257 s $\nu_{as}(SO_2)$, 1117 s $\nu_s(SO_2)$.

^{1}H NMR (DMSO-d_6), δ, ppm: 2.30 (s, 3 H, CH_3), 2.33 (s, 3 H, CH_3), 4.09 (q, 1 H, CH_3O*H*, ^3J = 16.3 Hz), 4.18 (d, 3 H, C*H*$_3$OH, ^3J = 16.3 Hz), 6.70–7.84 (m, 13 H_{arom}), 8.45 (s + d, $^3J_{Cd-H}$ = 24.6 Hz, 1 H, C*H*=N).

Electrosynthesis of the complexes was carried out by a standard classical procedure [22] using an EG&GPAR/173 potentiostat in a methanol–acetonitrile (1 : 1) mixture with the platinum electrode as a cathode and metal sheets (Zn and Cd) as an anode. The working solution (25 mL) contained H_2L (0.001 mol) and Et_4NClO_4 (0.01 g) as a conducting additive. Electrolysis was carried out in a U-shape glass tube with undivided anodic and cathodic spaces at a current strength of 15 mA and an initial voltage of 12 V for 1.5 h. After the end of electrolysis, the formed precipitates of the complexes were filtered off, washed with hot isopropanol, and dried in vacuo.

The spectral and analytical data of the electrochemically and chemically synthesized compounds coincide. The ECS yields of complexes **I** and **II** are 73 and 78%, respectively.

Elemental analysis to C, H, and N was carried out on a Carlo Erba Instruments TCM 480 analyzer. The IR spectra of the samples in KBr pellets were recorded on a Nicolet Impact-400 instrument in a range of 4000–400 cm^{-1}. The melting point was measured on a Koffler table. ^{1}H NMR spectra were recorded on a Varian Unity 300 spectrometer with a working frequency of 300 MHz in the regime of internal stabilization of the 2H polar resonance line in DMSO-d_6 at 20°C. Absorption spectra were recorded on a Cary 100 spectrophotometer (Varian). Fluorescence measurements were carried out on a Cary Eclipse spectrofluorimeter (Varian) using DMSO (spectral purity grade, Aldrich) to prepare solutions.

X-ray absorption spectroscopy. The X-ray absorption Zn *K* edge of compound **I** was obtained on the Structural Materials Science station at the Kurchatov Center of Synchrotron Radiation and Nanotechnologies (Moscow) [23]. The EXAFS (extended X-ray absorption fine structure) spectrum was processed using standard procedures of background isolation, normalization to the jump of the Zn *K* edge, and

atomic absorption (μ_0) isolation [24], after which the Fourier transformation of the isolated EXAFS (χ) spectrum was performed in the range of wave vectors of photoelectrons k from 2.6 to 12–13 Å^{-1} with the weight function k^3. The obtained module Fourier transformant (MFT) of EXAFS corresponded to the radial function of the atomic distribution around the absorbing zinc ion with the accuracy to the phase shift. The exact values for parameters of the nearest environment of the zinc ion in the studied compound were determined by the nonlinear fitting of the parameters of the corresponding coordination spheres by the comparison of the calculated EXAFS spectrum and that isolated from the full absorption spectrum using the Fourier filtration method. This nonlinear fitting was performed using the IFFEFIT program package [25]. The phases and scattering amplitudes of the photoelectron wave necessary for the construction of the model spectrum were calculated using the FEFF7 program [26].

The X-ray diffraction analysis of complex **II** was carried out on an Agilent Technologies Xcalibur E diffractometer equipped with a CCD detector and a monochromatic radiation source (MoK_α radiation, $\lambda = 0.71073$ Å) using the CrysAlisPro standard procedure [27]. The structure was solved by a direct method and refined in the full-matrix anisotropic approximation for all non-hydrogen atoms. The hydrogen atoms in complex **II** were localized from the difference electron density syntheses and refined in the isotropic approximation. The main crystallographic data for complex **II** the refinement parameters are presented in Table 1. All calculations were performed using the SHELXS-97 program package [28]. The full array of X-ray diffraction data was deposited with the Cambridge Crystallographic Data Centre (CIF file CCDC no. 1471159; deposit@ccdc.cam.ac.uk or http://www.ccdc.cam.ac.uk/data_request/cif).

The single crystals of complex **II** for X-ray diffraction analysis were obtained by the slow evaporation of the complex in a methanol–acetonitrile (1 : 1) mixture.

Table 1. Crystallographic data and the experimental and refinement characteristics for complex **II**

Parameter	Value
Empirical formula	$C_{50}H_{48}Cd_2N_8O_6S_4$
FW	1210.00
Crystal size, mm	0.32 × 0.16 × 0.11
Temperature, K	153(2)
Crystal system	Triclinic
Space group	$P\bar{1}$
a, Å	8.9292(5)
b, Å	10.2132(6)
c, Å	14.5173(8)
α, deg	91.0299(8)
β, deg	105.6954(7)
γ, deg	108.4688(7)
V, Å^3	1201.09(12)
Z	1
ρ_{calcd}, g/cm^3	1.673
μ, mm^{-1}	1.119
F(000)	612
θ ranges, deg	1.47–29.11
Ranges of reflection indices	$-12 \le h \le 12$, $-13 \le k \le 13$, $-19 \le l \le 19$
Number of measured reflections	13266
Number of independent reflections	6368
Number of reflections with $I > 2\sigma(I)$	5783
Number of refined parameters	322
GOOF (all reflections)	1.001
R_1 ($I > 2\sigma(I)$)	0.0280
wR_2 (all reflections)	0.0871
$\Delta\rho_{max}/\Delta\rho_{min}$, e Å^{-3}	0.681/–0.571

RESULTS AND DISCUSSION

Through the earlier works [29, 30] on the study of the complexation ability of the tosylamino-functionalized 5-hydroxypyrazole-containing tridentate Schiff base with Zn^{2+}, Cu^{2+}, Co^{2+}, and Ni^{2+} ions, we carried out the CS and ECS of the zinc and cadmium chelates with the sulfur-containing analog of the Schiff base H_2L in a methanol–acetonitrile solution (scheme).

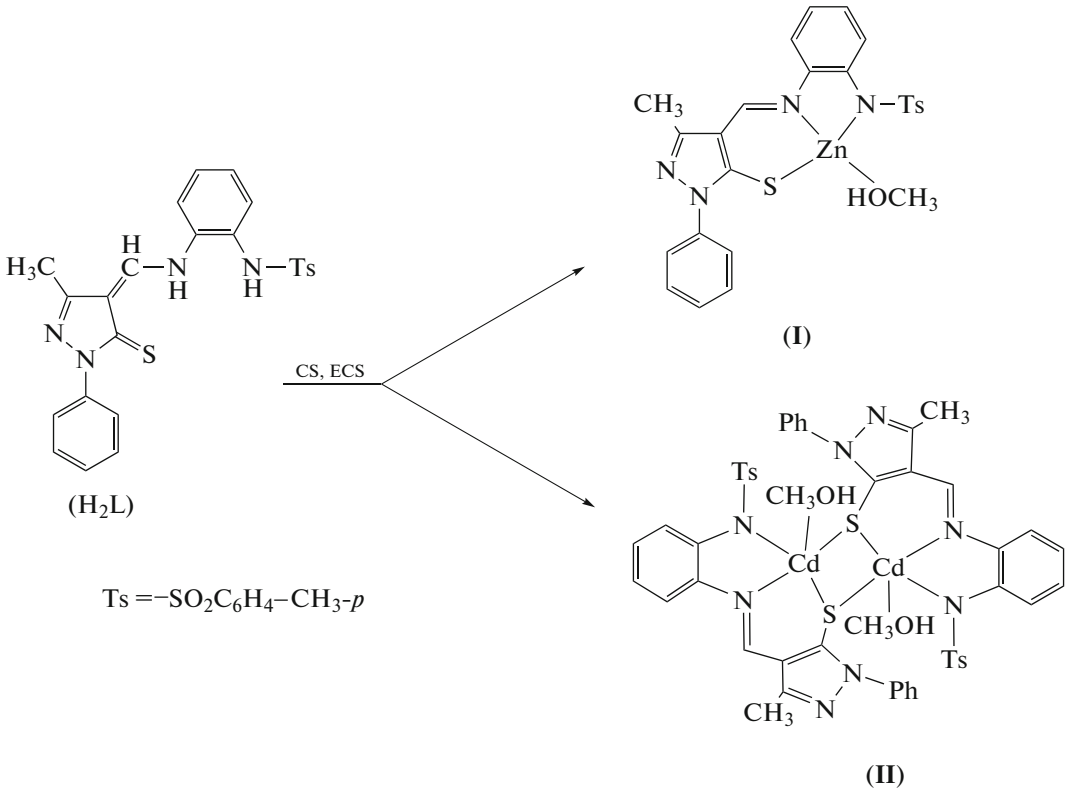

The overall complex formation process in the electrolytic cell can be presented as follows:

$(-)Pt/CH_3OH/CH_3CN + H_2L/M(+)$, M = Zn, Cd.

The ECS of the zinc complex is the following:

Cathode: $H_2L + 2e \rightarrow L^{2-} + H_2$.

Anode: $Zn^0 + L^{2-} + CH_3OH \rightarrow ZnL \cdot CH_3OH + 2e$.

The ECS of the cadmium complex is the following:

Cathode: $2H_2L + 4e \rightarrow 2L^{2-} + 2H_2$.

Anode: $2Cd^0 + 2L^{2-} + 2CH_3OH \rightarrow Cd_2L_2 \cdot 2CH_3OH + 4e$.

Several tautomers can be formed for H_2L as for its oxygen analog [29]. According to the IR and ^{1}H NMR spectral data, the thioenamine form is most stable in both the solution and solid state (scheme). The IR spectrum of H_2L exhibits an intense band of stretching vibrations of the vinylogic thioamide group C(=S)–CH=CHN at 1638 cm^{-1} [31], a ν(N–H) stretching vibration band at 3215 cm^{-1}, and asymmetric and symmetric stretching vibrations ν(SO_2) of the tosyl fragment at 1324 and 1154 cm^{-1}, respectively. The ^{1}H NMR spectrum recorded in DMSO-d_6 contains doublet signals from the proton of the CH and NH groups of the aminomethylene fragment C*H*N*H* at 8.67 and 14.49 ppm, respectively, with the vicinal spin-spin coupling constants ^3J = 12.4 Hz.

As compared to the IR spectrum of noncoordinated azomethine H_2L, the IR spectra of complexes **I** and **II** exhibit the disappearance of the band of ν(N–H) stretching vibrations of the tosylated amino group at 3215 cm^{-1} and vibrations of the vinylogic thioamide group C(=S)–CH=CHN at 1638 cm^{-1} and the disappearance of bands of ν(C=N) stretching vibrations of the azomethine group at 1618 and 1612 cm^{-1} for complexes **I** and **II**, respectively.

The disappearance of the doublet signals of the aminomethylene fragment and the appearance of the singlet signal of the C*H*=N proton of the imino group at 8.72 ppm are observed in the ^{1}H NMR spectra (DMSO-d_6) of zinc complex **I**. In addition, the ^{1}H NMR spectrum of complex **I** contains signals of coordinated methanol: a quartet from the proton of the hydroxyl group at 3.89 ppm and a doublet from the methyl group at 4.02 ppm with the vicinal constant ^3J = 14.7 Hz. Along with the aforementioned changes (the quartet of the methyl group at 4.09 and the doublet at 4.18 ppm with ^3J = 14.7 Hz of coordinated methanol), the spectrum of the cadmium complex exhibits signals from the *H*C=N protons of the imino group at 8.45 ppm with the characteristic constants

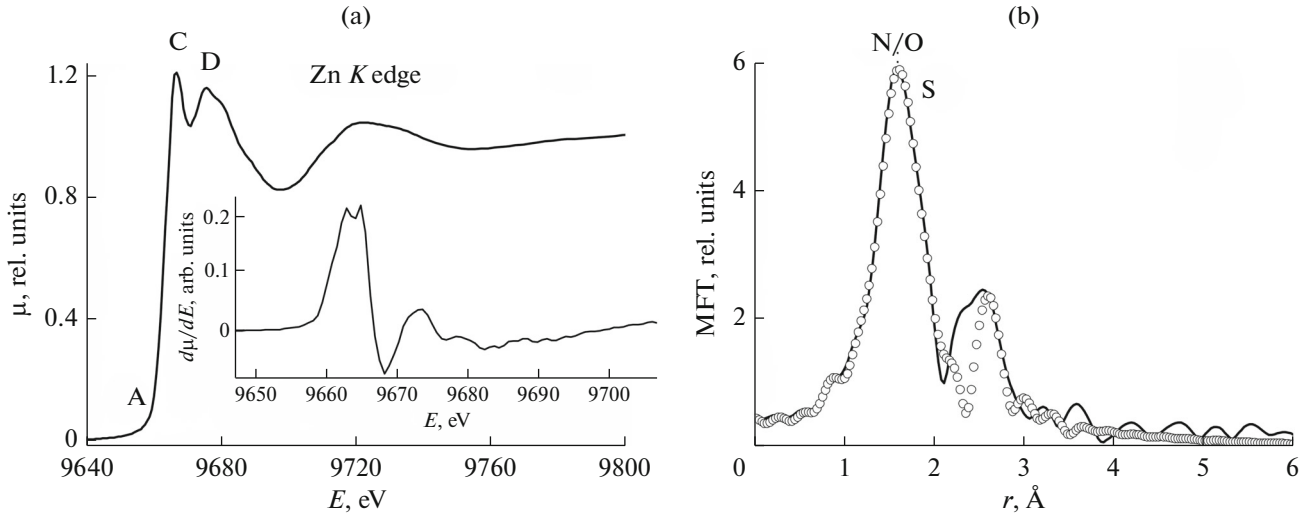

Fig. 1. (a) Normalized XANES and its first derivative and (b) MFT EXAFS Zn K-edge of comlex **I** (solid line: experimental, the open cycles show the best fit).

$^3J_{Cd-H}$ = 24.6 Hz, which additionally evidences for the formation of a bond of the nitrogen atom of the CH=N azomethine group with cadmium. Thus, both IR and NMR data favour a $\{MN_2OS\}$ coordination for the complexes **I** and **II** with participation of the imine nitrogen atom of the CH=N bond, the nitrogen atom of the tosylated amino group, the thiol sulfur atom, and oxygen of coordinated methanol.

The local atomic structure of complex **I** was determined by X-ray absorption spectroscopy. The data on the nearest atomic environment of the zinc ions in this compound were obtained from an analysis of the XANES (X-ray absorption near edge structure) and EXAFS Zn *K*-edge absorption. The X-ray Zn *K*-edge absorption and MFT EXAFS of complex **I** are shown in Fig. 1a. The XANES is presented by two major maxima (C, D), and the pre-edge structure (A) is absent because of the completely filled 3d shell of zinc(II). The first derivative of the Zn *K* edge also has two maxima, indicating the splitting of the free p* states of zinc cause by the low-symmetry environment of the zinc ions in the complex. The shapes of the Zn *K* edge and its first derivative are characteristic of the zinc complexes with the tetrahedral structure of the coordination sites of the molecules.

The quantitative characteristics of the local atomic structure of complex **I** were obtained from an analysis of the EXAFS Zn *K* edge of this compound. It is seen from Fig. 1b that the MFT EXAFS consists of the major peak at $r \approx 1.60$ Å unambiguously corresponding to the scattering on the nearest coordination spheres consisting of the nitrogen atoms of the ligands and the shoulder at $r = 1.84$ Å corresponding, most likely, to the scattering on the coordination sphere containing sulfur atoms. The less intense peaks at longer distances at $r = 2.3–2.5$ Å correspond to the scattering on the next coordination spheres of the ligands.

The parameters of the local atomic environment of the zinc ion in complex **I** obtained for the best model of the coordination polyhedron (the minimum value of the goodness-of-fit function ($\Re$) corresponds to this model) are presented in Table 2. Two nitrogen atoms are arranged at a medium distance of 2.01 Å, and one light atom (possibly, oxygen) of the additionally coordinated solvent (methanol) molecule is remote at a longer distance of 2.08 Å. Since the scattering amplitude of photoelectrons from the oxygen and nitrogen atoms is the same, these atoms cannot be distinguished in the first two coordination spheres. The coordination sphere consisting of one sulfur atom of the ligand is arranged at a distance of 2.29 Å. The subsequent MFT peaks correspond to the coordination sphere consisting of the carbon atoms of the ligands at the distances 2.87–3.00 Å. The values obtained for the Debye–Waller factor ($\sigma^2 = 0.0038–0.0045$ Å^2) are characteristic of the coordination spheres of this composition and radius.

Table 2. Parameters of the local atomic environment of the zinc ions in complex **I** obtained from the multisphere fitting of the EXAFS Zn *K*-edge absorption*

Compound	Coordination number	*R*, Å	σ^2, Å^2	Coordination sphere	GOOF, %
I	2	2.01	0.0038	N/O	2.9
	1	2.08	0.0038	N/O	
	1	2.29	0.0045	S	

* *R* are interatomic distances, σ^2 is the Debye–Waller factor, and GOOF is the goodness-of-fit function.

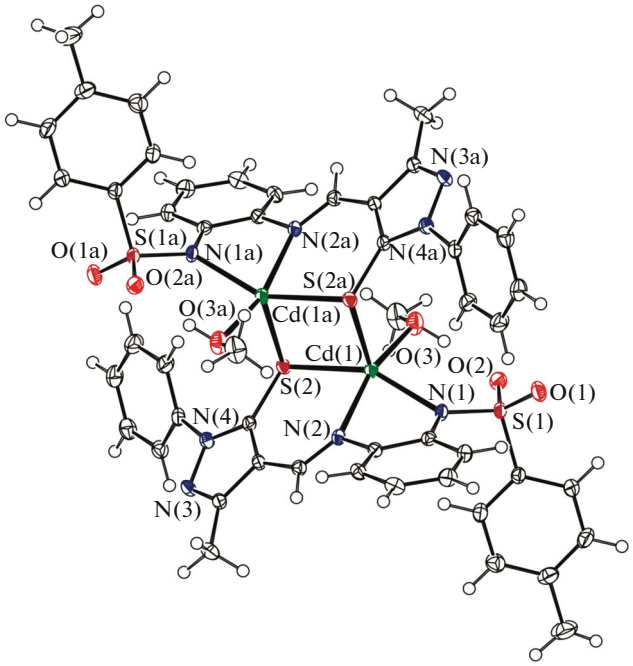

Fig. 2. Structure of dimeric complex **II** in representation of atoms by thermal shift ellipsoids with 50% probability.

The structure of dimeric cadmium chelate **II** was proved by X-ray diffraction analysis. The structural unit of complex **II** is the centrosymmetric dimer $[Cd(L)(CH_3OH)]_2$, whose general view is shown in Fig. 2. The S(2) atom of the mercaptopyrazole fragment performs the bridging function in the binuclear complex.

The coordination polyhedron of the cadmium atom is a distorted square pyramid. The dideprotonated residue of azomethine L^{2-} is coordinated to the Cd^{2+} ion through the tridentate coordination mode by the amine and azomethine nitrogen atoms (N(1) and N(2), respectively) and the S(2) atom of the mercaptopyrazole fragment. The fourth coordination site in the equatorial plane is occupied by the O(3) atom of the methanol molecule. The apical position is occupied by the S(2a) atom of the second monomeric fragment. The Cd(1)–S(2) and Cd(1)–S(2a) bond lengths are 2.6041(5) and 2.6367(5) Å, respectively. The Cd(1)S(2)Cd(1a) bond angle is 80.69(2)°, and the Cd(1)···Cd(1a) distance in the dimer is 3.3929(3) Å (Table 3).

The structure of the monomeric fragment $[CdL(CH_3OH)]$ is shown in Fig. 3. The azomethine ligand in the complex is not planar as a whole. The phenyl substituent is substantially turned relative to the pyrazole cycle. The dihedral angle between their mean planes is 41.43°. The benzene ring of the tosylamine fragment is also noncoplanar to the pyrazole cycle: the dihedral angle between their mean planes is 41.63°.

The five-membered chelate cycle Cd(1)N(1)C(1)C(6)N(2) has an envelope conformation, whose flap (Cd(1) atom) shifts from the mean plane of other atoms of the cycle by 0.867 Å. The six-membered metallocycle Cd(1)N(2)C(7)C(8)C(9)S(2) has a sofa conformation: the Cd(1) atom shifts from the mean plane of other atoms of the cycle by 0.381 Å.

The hydrogen atom of the methanol molecule forms the intramolecular hydrogen bond O(3)–

Table 3. Selected interatomic distances and bond angles in the coordination polyhedra of the cadmium atoms in the structure of complex **II***

Bond	*d*, Å	Bond	*d*, Å
Cd(1)–N(1)	2.2560(17)	Cd(1)–S(2)	2.6041(5)
Cd(1)–N(2)	2.2794(17)	Cd(1)–S(2)^{i}	2.6367(5)
Cd(1)–O(3)	2.2789(17)		
Angle	**ω, deg**	**Angle**	**ω, deg**
N(1)Cd(1)O(3)	97.29(6)	N(2)Cd(1)S(2)	89.83(4)
N(1)Cd(1)N(2)	73.82(6)	N(1)Cd(1)S(2)^{i}	103.14(5)
O(3)Cd(1)N(2)	162.51(7)	O(3)Cd(1)S(2)^{i}	103.82(5)
N(1)Cd(1)S(2)	152.71(5)	N(2)Cd(1)S(2)^{i}	92.98(4)
O(3)Cd(1)S(2)	92.15(5)	S(2)Cd(1)S(2)^{i}	99.31(2)

* Crystallographic positions: ^{i} $-x + 1, -y, -z + 1$.

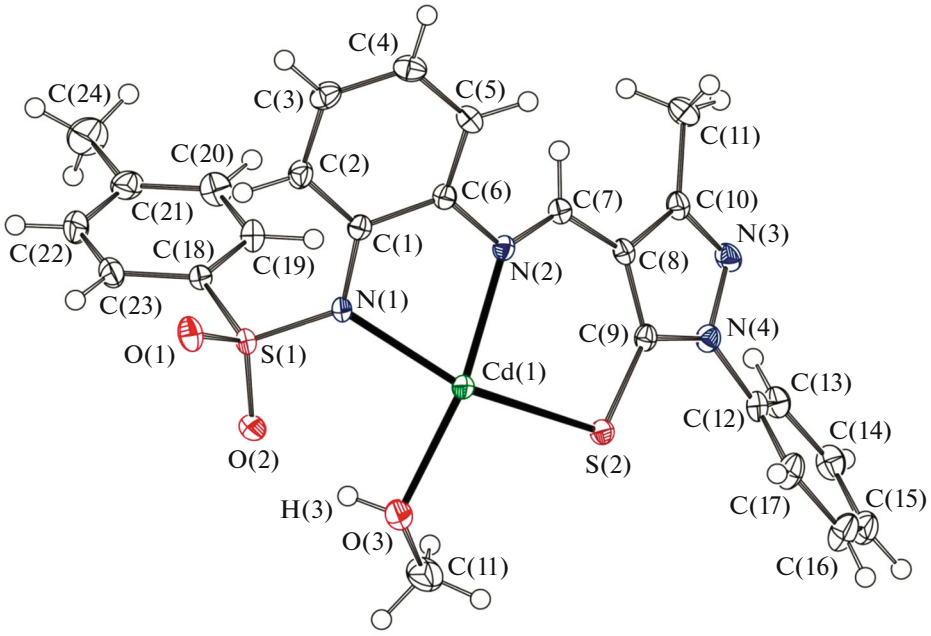

Fig. 3. Structure of the monomeric fragment of complex **II** in representation of atoms by thermal shift ellipsoids with 50% probability.

H(3)···O(2) with the O(2) atom of the tosyl fragment: D–H 0.866, H···A 1.831, D···A 2.660(3) Å, angle DHA 160°.

The optical and photoluminescence properties of H_2L and the related zinc (**I**) and cadmium (**II**) complexes were studied at room temperature in a DMSO solution. The data obtained are given in Table 4.

The electronic absorption spectra of solutions of compounds H_2L, **I**, and **II** are presented in Fig. 4.

The electronic absorption spectrum of H_2L in the spectral range from 300 to 550 nm is characterized by two absorption bands with maxima at 338 and 432 nm and molar absorption coefficients at the maxima of these bands of 16500 and 8900 L mol^{-1} cm^{-1}, respectively (Table 4, Fig. 4). Unlike H_2L, complexes **I** and **II** exhibit one absorption band with a maximum at 394 nm in the same spectral range. The electronic absorption spectra of the complexes are characterized by similar in shape and position but noticeably different in intensity (ε = 15850 and 29400 L mol^{-1} cm^{-1} for **I** and **II**, respectively) long-wavelength absorption bands (Table 4, Fig. 4). Complex formation results in the hypsochromic shift of the maxima of the long-wavelength absorbance of complexes **I** and **II** by 38 nm compared to that of H_2L.

Neither H_2L, no its metal complexes **I** and **II** luminesce in a DMSO solution at room temperature.

ACKNOWLEDGMENTS

This work was carried out using the equipment of the Molecular Spectroscopy Shared Facility Center at the Southern Federal University (Rostov-on-Don, Russia) in the framework of the design part of the state program for 2016 (project no. 007-01114-16 PR 0256-

Table 4. Spectral absorption characteristics of compounds H_2L, **I**, and **II** in DMSO at 293 K

Compound	Absorbance	
	λ_{max}, nm	ε, L mol^{-1} cm^{-1}
H_2L	338 432	16500 8900
I	394	15850
II	394	29400

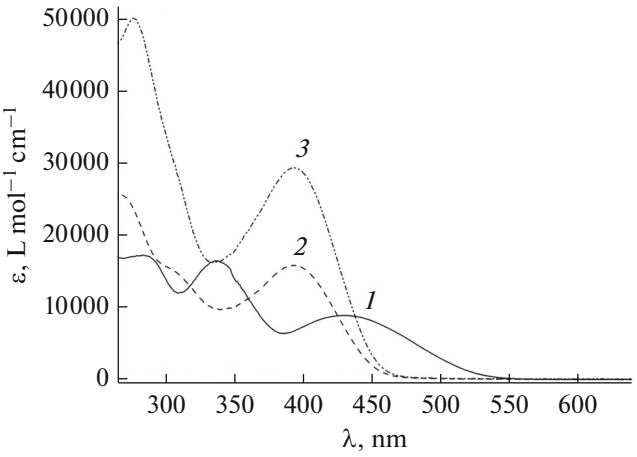

Fig. 4. Electronic absorption spectra of solutions of (*1*) ligand H_2L, (*2*) zinc complex **I**, and (*3*) cadmium complex **II** in DMSO.

2014-0009) and was supported by the President of the Russian Federation (grant no. NSh- 8201.2016.3).

REFERENCES

1. Garnovskii, D.A., Nivorozhkin, A.L., and Minkin, V.I., *Coord. Chem. Rev.*, 1993, vol. 126, p. 1.
2. Minkin, V.I., Nivorozhkin, L.E., and Korobov, M.S., *Usp. Khim.*, 1994, vol. 63, no. 4, p. 303.
3. Mistryukov, A.E., Vasilchenko, I.S., Sergienko, V.S., et al., *Mendeleev Commun.*, 1992, no. 1, p. 30.
4. Garnovskii, A.D. and Vasil'chenko, I.S., *Usp. Khim.*, 2005, vol. 74, no. 2, p. 193.
5. Nivorozhkin, A.L., Nivorozhkin, A.L., Minkin, V.I., et al., *Polyhedron*, 1991, vol. 10, no. 3, p. 179.
6. Toflund, H., Nivorozhkin, A.L., La Cour, A., et al., *Inorg. Chim. Acta*, 1995, vol. 228, p. 237.
7. Antsyshkina, A.S., Porai-Koshits, M.A., Vasil'chenko, I.S., et al., *Dokl. Ross. Akad. Nauk*, 1993, vol. 330, no. 1, p. 54.
8. Antsyshkina, A.S., Porai-Koshits, M.A., Nivorozhkin, A.L., et al., *Inorg. Chim. Acta*, 1991, vol. 180, no. 2, p. 151.
9. Takhirov, T.G., D'yachenko, O.A., Tagiev, D.B., et al., *Koord. Khim.*, 1988, vol. 14, no. 2, p. 237.
10. Uraev, A.I., Nivorozhkin, A.L., Korshunov, O.Yu., et al., *Russ. J. Coord. Chem.*, 1999, vol. 25, no. 1, p. 74.
11. Uraev, A.I., Nivorozhkin, A.L., Bondarenko, G.I., et al., *Dokl. Ross. Akad.* Nauk, 1999, vol. 367, no. 1, p. 67.
12. Uraev, A.I., Nivorozhkin, A.L., Bondarenko, G.I., et al., *Izv. Akad. Nauk, Ser. Khim.*, 2000, no. 11, p. 1863.
13. Uraev, A.I., Vlasenko, V.G., Kharisov, B.I., et al., *Polyhedron*, 2000, vol. 19, nos. 22–23, p. 2362.
14. Vlasenko, V.G., Uraev, A.I., Zubavichus, Ya.V., et al., *Bull. Russ. Acad. Sci. Phys.*, 2008, vol. 72, p. 468.
15. Nivorozhkin, A.L., Uraev, A.I., Bondarenko, G.I., et al., *J. Chem. Soc., Chem. Commun.*, 1997, no. 18, p. 1711.
16. Burlov, A.S., Uraev, A.I., Garnovskii, D.A., et al., *J. Mol. Struct.*, 2014, vol. 1064, p. 111.
17. Uraev, A.I., Popov, L.D., Levchenkov, S.I., et al., *Russ. J. Coord. Chem.*, 2014, vol. 40, no. 9, p. 599.
18. Levchenkov, S.I., Shcherbakov, I.N., Popov, L.D., et al., *J. Struct. Chem.*, 2015, vol. 56, no. 1, p. 113.
19. Levchenkov, S.I., Shcherbakov, I.N., Popov, L.D., et al., *J. Struct. Chem.*, 2015, vol. 56, no. 1, p. 113.
20. Kvitko, I.Ya., *Zh. Org. Khim.*, 1969, vol. 5, no. 7, p. 1685.
21. Malick, W.U. and Sharma, T.S., *J. Ind. Chem. Soc.*, 1970, vol. 47, no. 2, p. 167.
22. Tuck, D.G., *Pure Appl. Chem.*, 1979, vol. 51, no. 10, p. 2005.
23. Chernyshov, A.A., Veligzhanin, A.A., and Zubavichus, Y.V., *Nucl. Instr. Meth. Phys. Res. A*, 2009, vol. 603, p. 95.
24. Kochubei, D.I., Babanov, Yu.A., Zamaraev, K.I., et al., *Rentgenospektral'nyi metod izucheniya struktury amorfnykh tel: EXAFS-spektroskopiya* (X-Ray Spectral Method for Structure Investigation of Amorphous Solids: EXAFS Spectroscopy), Novosibirsk: Nauka SO, 1988.
25. Newville, M., *J. Synchrotron Rad.*, 2001, no. 8, p. 96.
26. Zabinsky, S.I., Rehr, J.J., Ankudinov, A., et al., *Phys. Rev.*, 1995, vol. 52, p. 2995.
27. *CrysAlisPro. Version 1.171.36.32*, Agilent Technologies (release 02-08-2013).
28. Sheldrick, G.M., *Program for the Refinement of Crystal Structure*, Göttingen: Univ. of Göttingen, 1997.
29. Garnovskii, D.A., Antsyshkina, A.S., Sadikov, G.G., et al., *Russ. J. Inorg. Chem.*, 2014, vol. 59, no. 5, p. 431.
30. Garnovskii, D.A., Antsyshkina, A.S., Makarova, N.I., et al., *Russ. J. Inorg. Chem.*, 2015, vol. 60, no. 12, p. 1528.
31. Kurkovskaya, L.N., Shapet'ko, N.N., Kvitko, I.Ya., et al., *Zh. Org. Khim.*, 1974, vol. 10, no. 10, p. 2210.

Translated by E. Yablonskaya